engineering proceedings

MDPI

Proceeding Paper

Validate CFD Simulation of H-Darrieus Vertical Axis Wind Turbine (VAWT) with Experimental Data †

M. Hikmatul Ridho * and Prabowo

Department of Mechanical Engineering, Sepuluh Nopember Institute of Technology, Surabaya 60111, East Java, Indonesia

* Correspondence: hikmatulridho98@gmail.com; Tel.: +62-822-6418-9024

† Presented at the 8th Mechanical Engineering, Science and Technology International Conference, Padang Besar, Perlis, Malaysia, 11–12 December 2024.

Abstract: The energy consumption pattern in the world, and in Indonesia today, is still dominated by fossil energy in oil, gas, and coal. It contradicts the reduced production of fossil energy, especially petroleum. Therefore, the government is trying to increase the role of new and renewable energy. One of the renewable energy sources that can be developed is wind energy. Indonesia has the potential for wind energy of 60.6 GW with an average wind velocity of 3–6 m/s. Given these conditions, it is expected that the installation of vertical axis wind turbines (VAWT) in buildings in urban areas and remote islands will be able to take advantage of the wind speed flowing above or beside buildings or skyscrapers, where the wind conditions do not have obstacles such as trees, houses, and so on. As a result, analysis and experimentation are required to design a wind turbine with good performance that can be used in cities or remote islands at relatively low wind speeds. The method used in this study is numerical analysis with computational fluid dynamics (CFD) with poly-hexacore meshing type, and the geometry sample is an H-Darrieus turbine. The input parameter is wind speed, which ranges from 2.5 to 9 m/s. The final goal of this study is to determine whether the CFD simulation modeling used is credible or valid.

Keywords: new and renewable energy (NRE); vertical axis wind turbine (VAWT); H-Darrieus wind turbine; wind turbine performance; wind energy; wind velocity; potential wind energy in Indonesia; numerical analysis; computational fluid dynamics (CFD)

check for updates

Academic Editors: Noor Hanita Abdul Majid, Agus Dwi Anggono, Waluyo Adi Siswanto, Tri Widodo Besar Riyadi, Mohammad Sukri Mustapa, Nur Rahmawati Syamsiyah and Afif Faishal

Published: 11 February 2025

Citation: Ridho, M.H.; Prabowo. Validate CFD Simulation of H-Darrieus Vertical Axis Wind Turbine (VAWT) with Experimental Data. *Eng. Proc.* **2025**, *84*, 53. https://doi.org/10.3390/engproc2025084053

Copyright: © 2025 by the authors. Licensee MDPI, Basel, Switzerland. This article is an open access article distributed under the terms and conditions of the Creative Commons Attribution (CC BY) license (https://creativecommons.org/licenses/by/4.0/).

1. Introduction

Energy needs globally continue to increase over time, as do energy needs in Indonesia. However, both globally and in Indonesia, energy consumption is still dominated by fossil fuels such as oil, gas, and coal [1].

This reliance on fossil fuels contradicts the decreasing production of these resources, especially petroleum. Consequently, the government is endeavoring to increase the role of New and Renewable Energy (NRE) sources [2].

Rising energy consumption trends are owing to constant population expansion and economic growth. In 2024, Indonesia's population will be 281,603.8 million, up from 278,696.2 million in 2023 [3].

Indonesia is an archipelagic nation with a sizable population and a massive land area. This is a challenge on its own for the Indonesian government, especially in making efforts to create equitable development by providing energy access for communities, especially

in remote areas, borders, and small islands. The electrification ratio is one of the primary metrics that the government uses to assess Indonesia's electricity supply's reach [4].

The electricity supply crisis in several areas, especially in remote and isolated areas, has had an unfavorable effect on Indonesia's economic growth. To overcome this, the Indonesian government is trying to create alternative power plants based on new and renewable energy (NRE), which utilize renewable resources such as wind, sunlight, and others. Indonesia has a wide range of energy sources, so there is a lot of room for new renewable energy (NRE), especially wind energy [5,6].

The potential of wind energy in Indonesia is quite exciting and promising for continued growth. Since Indonesia has a 154.6 GW wind energy potential, with 60.4 GW of that potential occurring onshore and 94.2 GW occurring offshore, with an average wind velocity of 3–6 m/s, some locations in Indonesia have the potential for wind speeds exceeding 6 meters per second. These locations include NTT, West Java, South Sulawesi, Maluku, and East Java [6].

Installing vertical axis wind turbines (VAWTs) in urban buildings and remote islands can harness wind speeds above or beside structures, free from obstacles like trees and houses [7]. Thus, this can fulfill the Indonesian government's commitment to reducing the effects of greenhouse gases (GHG) and achieving net zero emissions (NZE) by 2060. It also aligns with the government's plans, which include the usage and development of new and renewable energy (NRE) [5].

2. Basic Theory of VAWT Performance

Wind energy is a renewable energy source that may be used to generate electrical energy without the usage of fuel and can be deployed in a small space [6].

There are numerous factors to consider while designing a wind turbine, including how much power is required, wind speed, rotor diameter, and, as essential, how many blades must be employed, among other technical details [1,8].

Therefore, the energy that can be produced per unit of time is given by the formula below (Figure 1):

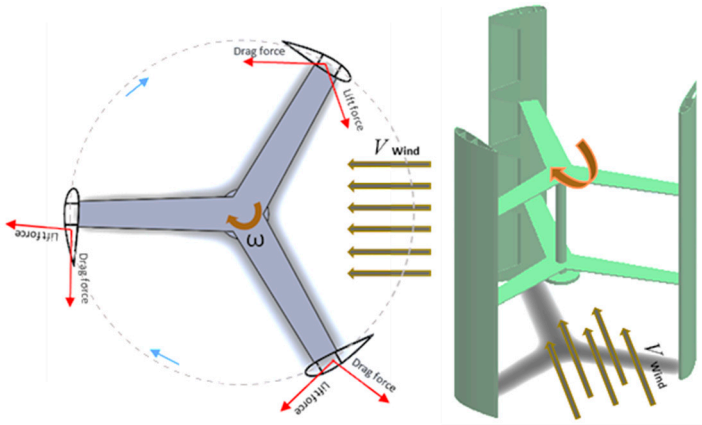


Figure 1. H-Darrieus turbine simple concept.

Tip speed ratio (λ) is the ratio between the rotating speed of the turbine and the wind speed. TSR is denoted by λ. To count the TSR, the following equation can be used:

$$\lambda = \frac{\omega . R}{v_w} \quad (1)$$

where:

λ = tip speed ratio (TSR)

ω = turbine angular velocity (rad/s)
R = turbine radius (m)
V_w = wind velocity (m/s)

The fluid flow mechanism greatly influences turbine performance through the type of flow received by the turbine. In this case, the influence of the Reynolds number greatly dominates in producing the force that occurs in the H-Darrieus wind turbine, and the definition of the Reynolds number is the ratio of inertial force to viscous force and is a simple parameter to estimate if a flow condition will be laminar or turbulent.

$$\mathrm{Re} = \frac{Inersia\ force}{viscous\ force} = \frac{\rho.V.L}{\mu} = \frac{V.L}{v} \tag{2}$$

where:

Re = Reynolds number
L = characteristic length (m)
ρ = wind density (kg/m^3)
μ = dynamic/absolute viscosity (N.s/m^2)
v = kinematic viscosity (m^2/s)
V = flow free stream speed (m/s)

Meanwhile, to find the moment coefficient for each turbine blade, you must first determine the swept area with the equation below:

$$\mathrm{A} = D \times H \tag{3}$$

where:

A = swept area/aspect ratio
H = rotor height (m)
D = turbine diameter (m)

Swept area is used as a reference value in computational fluid dynamics (CFD) to calculate the moment coefficient. To calculate the non-dimensional moment coefficient, use Equation (7) below:

$$Cm = \frac{T}{\frac{1}{4}\rho A D V^2} \tag{4}$$

where:

T = torque (Nm)
ρ = density of air mass (kg/m^3)
A = swept area/aspect ratio (m^2)
V = air speed (m/s)

Meanwhile, the non-dimensional term to compare the efficiency of the vertical axis wind turbine (VAWT) is the power coefficient. The power coefficient is the comparison or ratio between the power produced by the H-Darrieus turbine and the maximum wind power for the same swept area.

The power coefficient can then be calculated using the equation below:

$$CP = \frac{PT\ \omega}{\frac{1}{2}\ \rho\ A\ v^3} \tag{5}$$

$$CP = \frac{T\ \omega}{\frac{1}{2}\ \rho\ A\ v^3} \tag{6}$$

$$CP = \lambda c_m \tag{7}$$

where:

P = power in watt (W)

From this equation, it can be seen that the power coefficient is obtained from the results of the tip speed ratio and the moment coefficient.

3. Numerical Simulations

Numerical simulation is a method that uses digital models to study the mechanics of complex structures. This simulation is carried out by combining digital models of various aspects of the system to create a complete system model.

3.1. Computational Fluid Dynamics (CFD) Theory

The process of transforming fluid dynamics governing equations from the integral and derivative form into discretized algebraic form so that a computer can solve them and determine the flow field's values at specific discrete places or times is known as computational fluid dynamznergy equation are the three governing equations in fluid dynamics.

Integral form of the continuity equation,

$$\frac{\partial}{\partial t}\int\int\int_{V}\rho dV + \int\int_{A}\rho\vec{V}\cdot d\vec{A} = 0 \tag{8}$$

Differential form of the continuity equation,

$$\frac{\partial \rho}{\partial t} + \rho\vec{\nabla}\cdot\vec{V} = 0 \tag{9}$$

Momentum equation along the x-axis,

$$\frac{\partial(\rho u)}{\partial t} + \vec{\nabla}\cdot\left(\rho u\vec{V}\right) = -\frac{\partial p}{\partial x} + \frac{\partial \tau_{xx}}{\partial x} + \frac{\partial \tau_{yx}}{\partial y} + \frac{\partial \tau_{zx}}{\partial z} + \rho f_x \tag{10}$$

Momentum equation along the y-axis,

$$\frac{\partial(\rho v)}{\partial t} + \vec{\nabla}\cdot\left(\rho v\vec{V}\right) = -\frac{\partial p}{\partial y} + \frac{\partial \tau_{xy}}{\partial x} + \frac{\partial \tau_{yy}}{\partial y} + \frac{\partial \tau_{zy}}{\partial z} + \rho f_y \tag{11}$$

Momentum equation along the z-axis,

$$\frac{\partial(\rho w)}{\partial t} + \vec{\nabla}\cdot\left(\rho w\vec{V}\right) = -\frac{\partial p}{\partial z} + \frac{\partial \tau_{xz}}{\partial x} + \frac{\partial \tau_{yz}}{\partial y} + \frac{\partial \tau_{zz}}{\partial z} + \rho f_z \tag{12}$$

The energy equation is written in terms of internal energy,

$$\frac{\partial}{\partial t}\left[\rho\left(e + \frac{V^2}{2}\right)\right] + \vec{\nabla}\cdot\left[\rho\left(e + \frac{V^2}{2}\right)\vec{V}\right] = \rho\dot{q} - \frac{\partial(\rho p)}{\partial x} - \frac{\partial(vp)}{\partial y} - \frac{\partial(wp)}{\partial z} + \rho\vec{f}\cdot\vec{V} \tag{13}$$

A continuous closed-form expression for the dependent variable across the whole domain is obtained by solving a partial differential analytical problem. Numerical equation solutions, on the other hand, can only provide values at specific locations inside the domain, also referred to as grid points.

3.2. Pre-Processing in CFD Simulations

The pre-processing stage is where the user sets up the simulation environment. This stage involves defining the geometry, mesh generation, and boundary conditions. Defining the geometry involves importing the 3D model of the object or system to be simulated. Details are as follows (Figures 2 and 3).

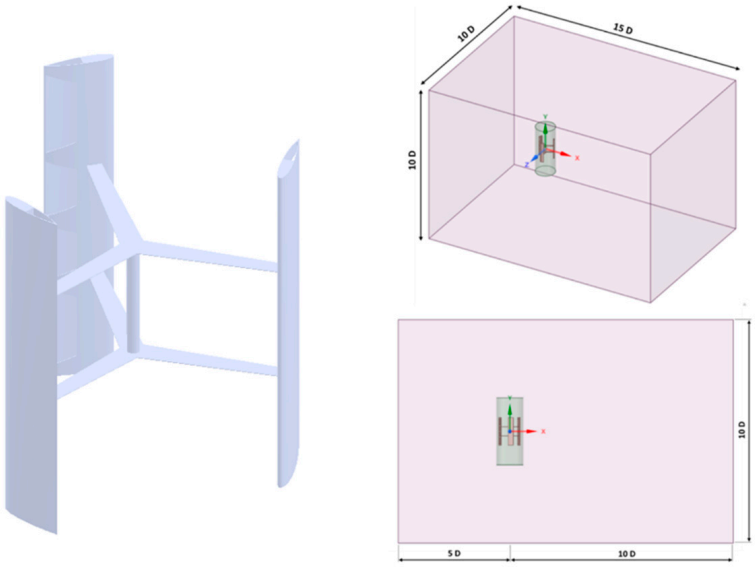


Figure 2. (**a**) Geometry of the H-Darrieus wind turbine. (**b**) The fluid computational domain in CFD simulation of the H-Darrieus turbine.

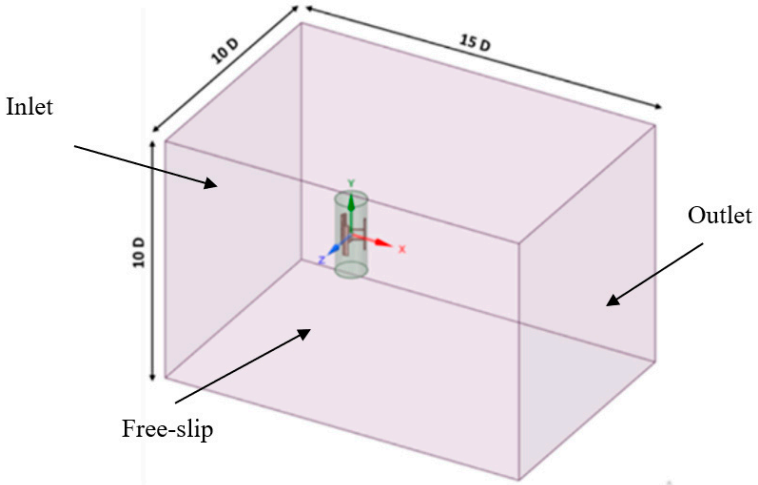


Figure 3. Boundary conditions in the computational domain.

3.3. Meshing

In CFD, meshing, or discretization, refers to the process of transforming a continuous fluid domain into a discrete computational domain so that fluid equations can be solved numerically, specifically using the computational fluid dynamics (CFD) approach [9,10].

In the CFD software, the resulting meshing is a hexahedron with high resolution and computational efficiency. Meanwhile, in the intricate regions, the mesh is polyhedral, which has the advantage of being able to track picture objects with high curvature. The total elements used in this simulation are 700 k elements (Figure 4).

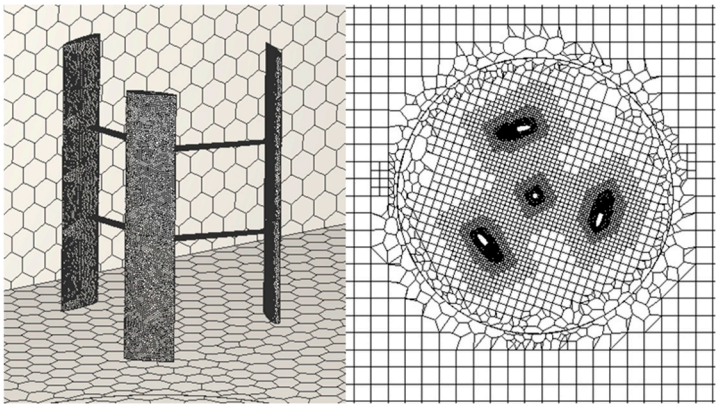


Figure 4. Mesh results in the computational domain.

3.4. Computing Settings

The simulation was carried out using CFD (computational fluid dynamics)-based software with the following settings:

(1) Transient

The simulation is carried out transiently with a simulation time step size of 0.01s.

(2) Turbulence: k-omega, SST

The SST equation can accommodate lengthy, straight fluid flows in straight pipes, but the k-omega equation improves accuracy in places with complex flow and near suction outlets.

(3) Inlet: velocity inlet

In the simulation, various inlet velocity values are used on the inlet surface.

(4) Pressure outlet (Outflow)

The outlet section defines a pressure outlet (outflow) to reflect the flow's "exit" within the computation domain.

(5) Moving Elements: 6 degrees of freedom

The 6 dof approach is utilized in this VAWT simulation, with the wind turbine's moment of inertia value of 0.9034497 kg/m^2. This number was calculated using the total weight of the three blades utilized, 5508 kg, and the wind turbine's radius of 0.405 m.

The fluid used in this simulation is incompressible air. Other settings not specified in the study are default settings that were not changed to maintain a conservative solution level.

4. Result and Discussion

This subchapter will provide the research findings, particularly the performance of the H-Darrieus turbine and the validation of CFD calculations by experimental data comparisons.

4.1. Performance Parameters

The wind speed range used in this research was 2.5 to 9 m/s, and the conditions were not loaded.

The H-Darrieus turbine's performance metrics include rpm vs time, power vs time, torque vs time, torque vs. tsr, and Cp vs tsr. Please see the details below.

In Figure 5, it can be concluded that as the wind speed increases over a certain time, the rpm will be higher.

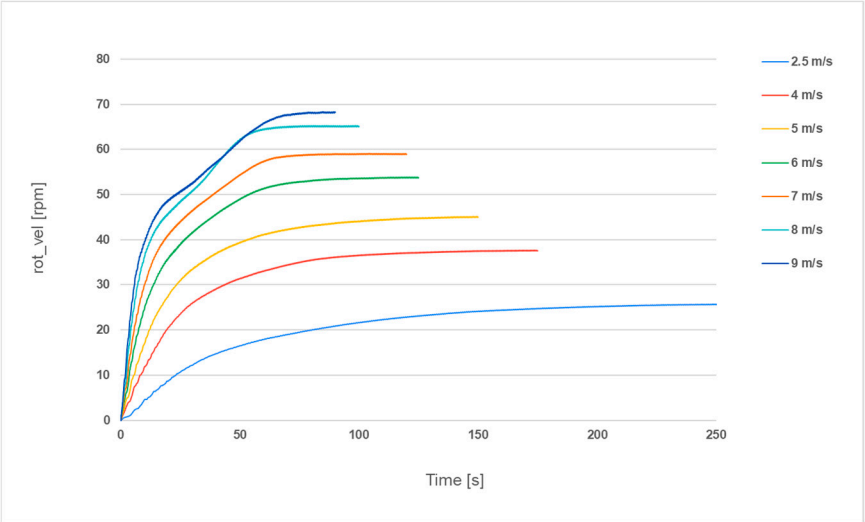


Figure 5. Graph illustrating turbine rotational speed over time as wind speed variations.

In Figures 6 and 7, torque and power numbers appear to remain constant over time, approaching zero, regardless of speed variance. This is due to the fact that the simulation in this study was performed in non-loading conditions.

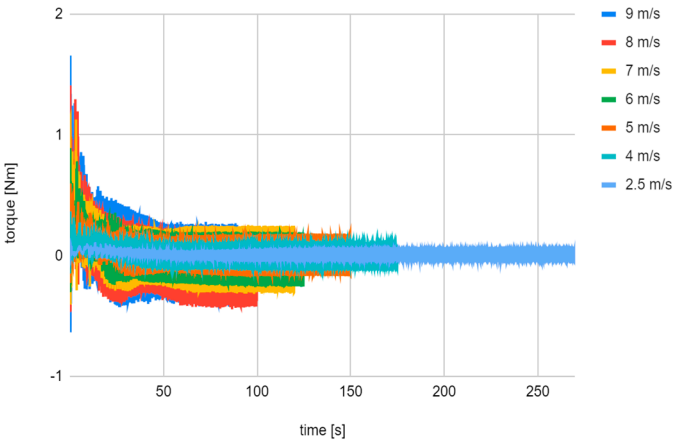


Figure 6. Graph illustrating turbine torque over time as wind speed variations.

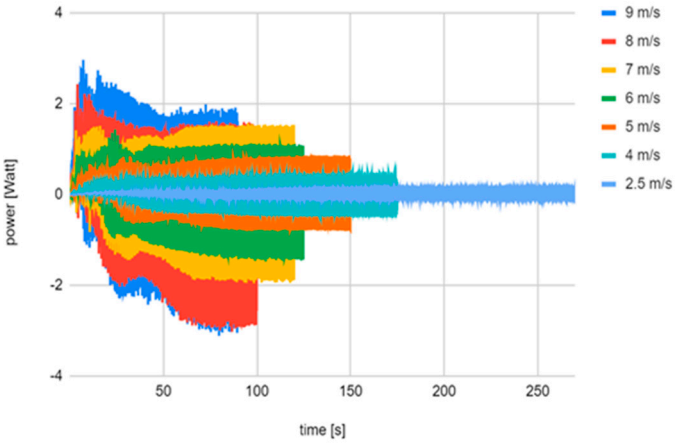


Figure 7. Graph illustrating turbine power over time as wind speed variations.

Figures 8 and 9 show that the torque and Cp values for TSR are consistent and close to zero. This is due to the fact that the simulation in this study was performed in non-loading conditions.

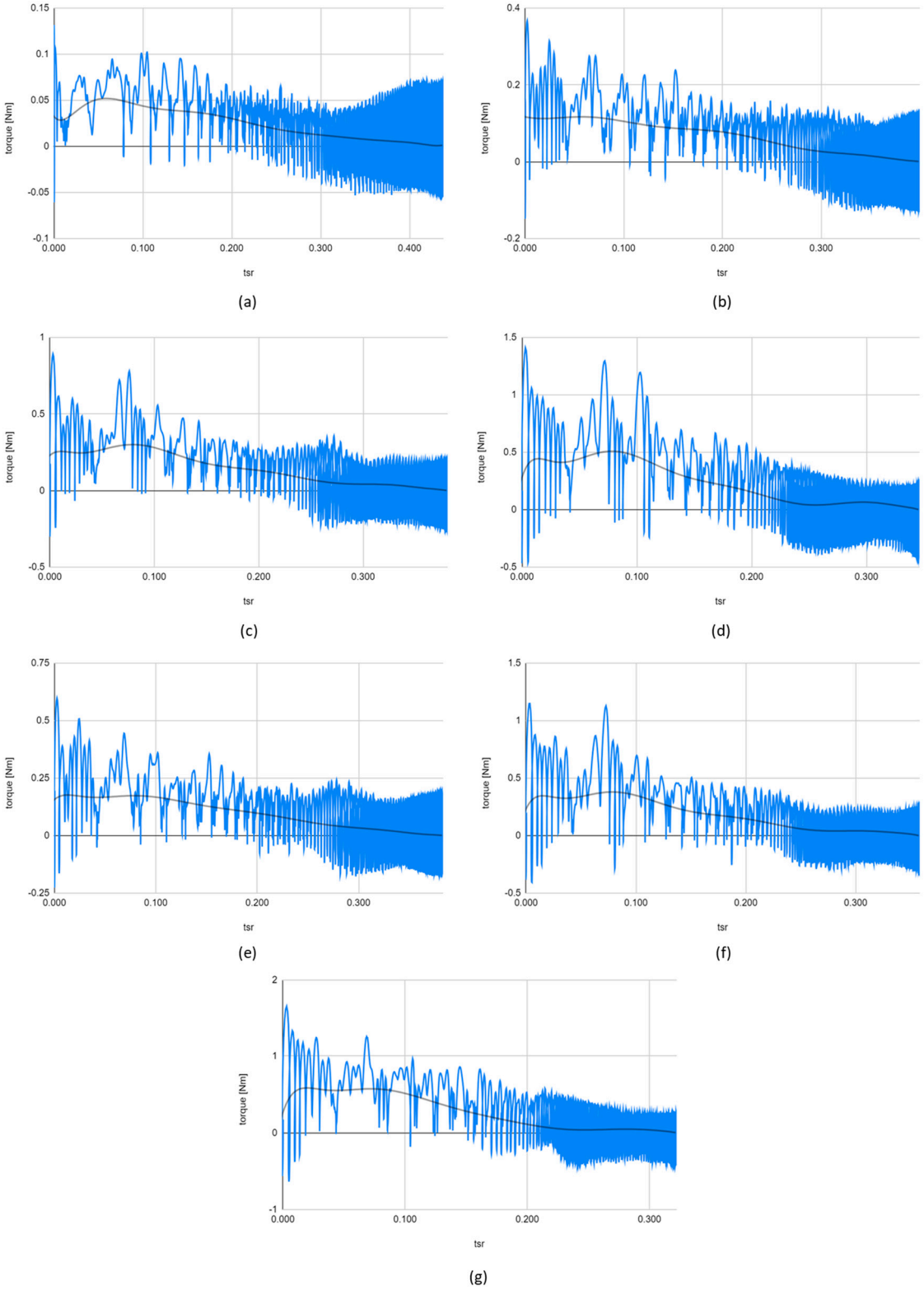


Figure 8. (**a**) Torque vs tsr at velocity 2.5 m/s; (**b**) torque vs tsr at velocity 4 m/s; (**c**) torque vs tsr at velocity 5 m/s; (**d**) torque vs tsr at velocity 6 m/s; (**e**) torque vs tsr at velocity 7 m/s; (**f**) torque vs tsr at velocity 8 m/s; (**g**) torque vs tsr at velocity 9 m/s.

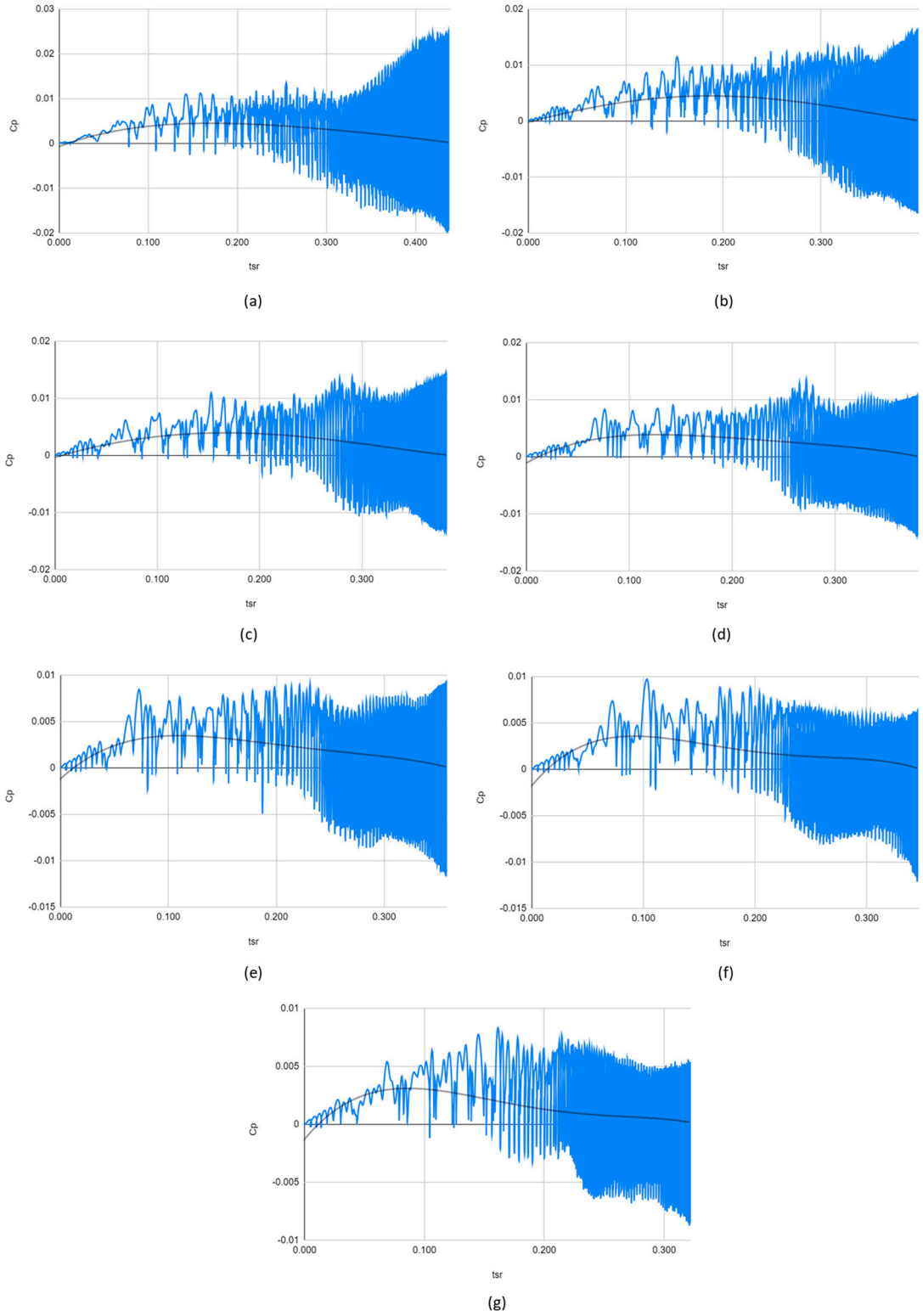


Figure 9. (**a**) Cp vs tsr at velocity 2.5 m/s; (**b**) Cp vs tsr at velocity 4 m/s; (**c**) Cp vs tsr at velocity 5 m/s; (**d**) Cp vs tsr at velocity 6 m/s; (**e**) Cp vs tsr at velocity 7 m/s; (**f**) Cp vs tsr at velocity 8 m/s; (**g**) Cp vs tsr at velocity 9 m/s.

4.2. Validation of Numerical Result

Validation in CFD simulation results will be compared with experimental results. Please see the details below.

Figure 10 depicts the rpm versus velocity graph under experimental and simulation circumstances. The CFD simulation results can be justified or said to be valid based on graphs (a) and (b), as shown in the bar diagram graph (b) at a wind speed of 4 m/s can produce an rpm of 37.56, and the bar graph (a) at a wind speed of 4.15 m/s can produce an rpm of 37.62.

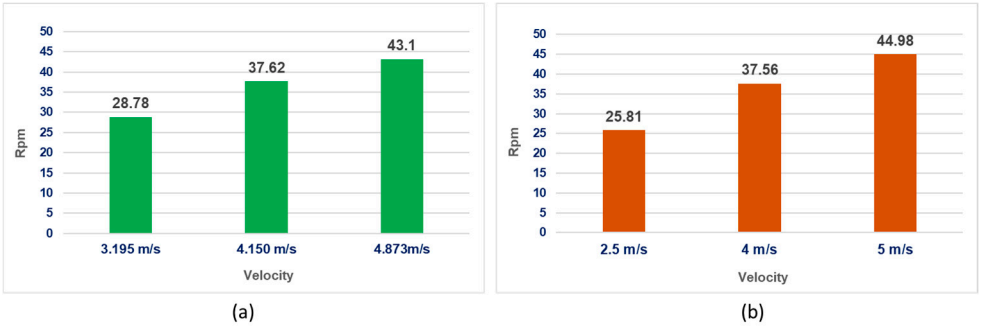


Figure 10. (**a**) Rpm vs velocity on experimental; (**b**) rpm vs velocity on CFD simulation.

Figure 10b is taken from Figure 5 with constant rpm parameters produced at speed variations of 2.5 m/s, 4 m/s, and 5 m/s.

With a wind speed parameter of 4 m/s (Figure 10b) and a wind speed of 4.15 m/s (Figure 10a), there is a very minor variation of 0.15 m/s, and the resulting rpm between the two has a difference. The little one is also 0.06, which is acquired by subtracting 37.62 from 37.56. The percentage error number for both is 0.9984, which is derived by dividing 37.56 by 37.62 and multiplying by 100%. This is also apparent at a speed of 2.5 m/s (Figure 10b) vs. 3,195 m/s (Figure 10a) and a speed of 5 m/s (Figure 10b) vs. 4.87 m/s (Figure 10). All have reasonable results, and the differences are not excessive. Thus, the CFD simulation in this study can be considered valid.

5. Conclusions

The CFD simulation results can be justified or said to be valid based on Section 4.2 "*Validation of Numerical Result*", especially in Figure 10a,b. With a relatively tiny error value of 0.9984 and a not-too-large variation in rpm value to wind speed, the CFD simulation in this study can be considered valid.

Lastly, in the actual application condition based on experimental and simulation data, the H-Darrieus turbine suitable to apply in Indonesia has an average wind speed of 3–6 m/s.

Author Contributions: Conceptualization, M.H.R. and P.; methodology, M.H.R.; software, M.H.R.; validation, M.H.R.; formal analysis, M.H.R.; investigation, M.H.R.; resources, M.H.R.; data curation, M.H.R.; writing—original draft preparation, M.H.R.; writing—review and editing, M.H.R.; visualization, M.H.R.; supervision, P.; project administration, M.H.R. and P.; funding acquisition, M.H.R. All authors have read and agreed to the published version of the manuscript.

Funding: This research received no external funding.

Institutional Review Board Statement: Not applicable.

Informed Consent Statement: Not applicable.

Data Availability Statement: The data presented in this study are available on request from the corresponding author.

Acknowledgments: The author would like to thank Prabowo who has provided learning opportunities and guidance in the Mechanical Engineering master's program, in Sepuluh Nopember Institute of Technology.

Conflicts of Interest: The authors declare no conflicts of interest.

References

1. Lei, H.; Zhou, D.; Lu, J.; Chen, C.; Han, Z.; Bao, Y. The impact of pitch motion of a platform on the aerodynamic performance of a floating vertical axis wind turbine. *Energy* **2017**, *119*, 369–383. [CrossRef]
2. Eltayesh, A.; Castellani, F.; Natili, F.; Burlando, M.; Khedr, A. Francesco Castellani. Aerodynamic upgrades of a Darrieus vertical axis small wind turbine. *Energy Sustain. Dev.* **2023**, *73*, 126–143. [CrossRef]
3. Central Bureau of Statistics (Indonesia). 2024. Available online: https://www.ceicdata.com.cn/en/indonesia/population-projection-by-province-central-bureau-of-statistics (accessed on 6 February 2025).
4. Setiawan, P.A.; Yuwono, T.; Widodo, W.A.; Julianto, E.; Santoso, M. Numerical Study of a Circular Cylinder Effect on the Vertical Axis Savonius Water Turbine Performance at the Side of the Advancing Blade with Horizontal Distance Variations. *Int. J. Renew. Energy Res.* **2019**, *9*, 978–985.
5. Ministry of Energy and Mineral Resources of the Republic of Indonesia (MEMR). Empat Kerjasama Menuju Net Zerro Emission Tahun 2060 Ditandatangani; 124. Pers/04/SJI/2022. 2022. Available online: https://www.esdm.go.id/id/media-center/arsip-berita/empat-kerjasama-menuju-net-zerro-emission-tahun-2060-ditandatangani (accessed on 6 February 2025).
6. Ministry of Energy and Mineral Resources of the Republic of Indonesia (MEMR). Wind Energy Development in Indonesia, Investment Plan, Final Report, 2024. Available online: https://www.energytransitionpartnership.org/wp-content/uploads/2024/09/20240906-Final-Report-Wind-Energy-Development-in-Indonesia-Investment-Plan-v2.0.pdf (accessed on 6 February 2025).
7. Roy, S.; Saha, U.K. Wind tunnel experiments of a newly developed two–bladed Savonius–style wind turbine. *Appl. Energy* **2015**, *137*, 117–125. [CrossRef]
8. Salleh, M.B.; Kamaruddin, N.M.; Mohamed-Kassim, Z. Experimental investigation on the effects of deflector angles on the power performance of a Savonius turbine for hydrokinetic applications in small rivers. *Energy* **2022**, *247*, 123432. [CrossRef]
9. Liu, Y.; Xiao, Q.; Incecik, A.; Peyrard, C. Aeroelastic analysis of a floating offshore wind turbine in platform-induced surge motion using a fully coupled CFD-MBD method. *Wind. Energy* **2018**, *2018*, 1–20. [CrossRef]
10. Saha, U.K.; Thotla, S.; Maity, D. Optimum design configuration of Savonius rotor through wind tunnel experiments. *J. Wind. Eng. Ind. Aerodyn.* **2008**, *96*, 1359–1375. [CrossRef]

Disclaimer/Publisher's Note: The statements, opinions and data contained in all publications are solely those of the individual author(s) and contributor(s) and not of MDPI and/or the editor(s). MDPI and/or the editor(s) disclaim responsibility for any injury to people or property resulting from any ideas, methods, instructions or products referred to in the content.